Characterization of strange attractors in spin-wave chaos

F. M. de Aguiar, A. Azevedo, and S. M. Rezende
Departamento de Física, Universidade Federal de Pernambuco, 50739, Recife, Pernambuco, Brazil
(Received 22 February 1988; revised manuscript received 6 September 1988)

We report the characterization of strange attractors in spin-wave chaos observed in microwave pumping experiments in yttrium iron garnet. Two types of scenarios are studied with parallel pumping and subsidiary resonance techniques. The dimension of the attractors at the onset of chaos is in all cases less than 2, indicating that few modes participate in the spin-wave chaotic dynamics.

INTRODUCTION

Microwave-pumped spin-wave instabilities in magnetic materials display a rich variety of nonlinear-dynamic phenomena such as self-oscillations, spiking, period multiplication, irregular period oscillations, intermittency, and chaos. The low-frequency oscillations with a variety of wave shapes have been known to exist[1] since the early days of the spin-wave pumping experiments.[2–4] For years the origin of the oscillations was not understood, until several authors[5] showed that they resulted from the nonlinear dynamics of spin waves pumped above the instability threshold. However, their extensive work fell short of connecting the spin-wave turbulence with the modern ideas of chaotic dynamics of nonlinear dissipative systems. In recent years there has been revival of interest in spin-wave turbulence. Chaotic dynamics has been studied in ferromagnetic[6–10] as well as antiferromagnetic[11–13] materials, in bulk form and in thin films,[14] and several theoretical papers[15–20] have been published on the subject.

Spin-wave nonlinearities are of particular interest because they can be modeled by nonlinear equations derived from microscopic Hamiltonians with well-known parameters, providing a theoretical framework to interpret the experimentally observed chaotic dynamics. The relevance of this is that in most other physical systems it is not possible to describe the nonlinearities by theoretical models based on microscopic systems parameters. In the usual experimental setup to investigate spin-wave turbulence, a magnetic sample is driven by a microwave rf field either parallel or perpendicular to the static magnetic field. The nonlinear dynamic effects are observed in the amplitude modulation which appears in the microwave field returning from the sample when the pumping is well above the instability threshold.[2–4] This modulation arises from the time variation in the magnon populations resulting from the dynamic interplay between parametric spin-wave modes. However, there is no direct experimental evidence of this, nor of the nature or the number of such modes. A model with two spin-waves modes[15] has successfully explained many features of the experimental results,[10,16,17] but it uses fictitious rather than realistic interaction parameters. Moreover several questions remain unanswered, such as the higher self-oscillation frequency predicted by theory as compared to the observed ones. One basic question that deserves attention regards the number of modes involved in the process, since it is expected that an entire manifold of modes is pumped above threshold.[18–20] Thus, despite the existence of a microscopic theoretical framework to treat spin-wave chaotic dynamics, a close correspondence between theory and experiment has not been achieved so far. Clearly, further theoretical and experimental effort is needed to achieve a full understanding of spin-wave chaos.

In order to gain understanding about the number of modes involved in spin-wave chaotic dynamics, we have performed microwave measurements to characterize the strange attractors of two routes to chaos previously observed in yttrium iron garnet (YIG). From time-series data the attractor dimensions and the metric entropies are calculated using an embedding technique. Two different algorithms are employed to calculate these quantities to ensure a more reliable characterization of the attractors.

EXPERIMENTAL RESULTS

The experiments reported here were performed at microwave pumping frequencies in the range 9.2–9.4 GHz. A spherical YIG sample with diameter 1.0 mm was held at room temperature in the center of a TE_{102} cavity ($Q \simeq 3000$) with the magnetic rf field either perpendicular (subsidiary resonance) or parallel to the applied dc field $\mathbf{H}_0$. The power was provided by a 2-W traveling-wave-tube amplifier fed by a backward-wave oscillator. Its frequency was stabilized with an external crystal oscillator and manually adjusted to the center of the cavity resonance. Microwave signals reflected from the cavity were converted down to 60 MHz, amplified, and monitored either with a spectrum analyzer or with a crystal detector. The resulting signals were then recorded in a storage oscilloscope. Time-series data were also stored in a computer at intervals of 0.2 μs using a commercial digitizer. At low power levels the signal reflected from the critically coupled cavity is negligible. As the driving field h is increased, an abrupt change in the signal occurs at the threshold value h_c for which a pump photon with frequency ω_p excites a pair of parametric magnons with

wave vectors $\mathbf{k}$ and $-\mathbf{k}$. The value of $\mathbf{k}$ is determined by the frequency ω_p, the field H_0 and the condition for minimum threshold, which depends on the pumping configuration. The main difference between the parallel pumping and the subsidiary resonance is that in the former process the magnon pair is driven directly by the incoming photon,[3,4] whereas in the latter it is mediated by the off-resonance $k=0$ magnon mode.[2] Due to the nature of the dipolar interaction, in the parallel pumping process the magnon pairs with minimum threshold have $\mathbf{k}\perp\mathbf{H}_0(\Theta_k=\pi/2)$ while in subsidiary resonance $\Theta_k=\pi/4$.[2] As h increases in the post threshold region the reflected microwave signal increases until it suddenly develops a low-frequency (50–500 kHz) amplitude modulation, corresponding to a Hopf bifurcation. The frequency, shape, and amplitude of this self-oscillation depend on the pumping configuration, crystal orientation with respect to $\mathbf{H}_0$, and the values of H_0 and $R\equiv h/h_c$. At an arbitrary orientation and field value, except for the gradual increase in self-oscillation frequency nothing dramatically happens as R increases. However, at conveniently selected configurations the low-frequency modulation shows period multiplication and chaos as R is increased.

Two clearly distinct scenarios of period multiplication have been observed both in the parallel[7] and transverse pumping[10] processes. The first scenario, which we call F henceforth, is a typical Feigenbaum route to chaos. The original self-oscillation with period T bifurcates to periods $2T$, $4T$, $8T$, and $16T$ with increasing control parameter R before it becomes chaotic. In the other scenario (C) there is only one period-doubling bifurcation before the onset of chaos. In this case in the transition to chaos the signal with period $2T$ seems to go through a narrow region of aperiodic oscillations, but there is no evidence of periods $4T$ or $8T$ as in scenario F. Figure 1 illustrates scenario F in the subsidiary resonance configuration with the sample oriented with the [100] direction along $\mathbf{H}_0$ and $H_0=1950$ Oe. A self-oscillation appears initially with 450 kHz at $R=2.12$ and its frequency gradually increases with R before period-doubling bifurcations occur at $R=2.19$ and $R=2.29$, leading to chaos at $R=2.54$. Period $8T$ was also clearly observed. Scenario C was observed in subsidiary resonance with the sample oriented with the [111] direction along $\mathbf{H}_0$ and $H_0=1980$ Oe. By increasing the driving power, regular, period $2T$ and noisy period $2T$ oscillations are observed as shown in Fig. 2, with no evidence of further bifurcations before the onset of chaos. In this case the subharmonic amplitude grows with increasing R, reaches a

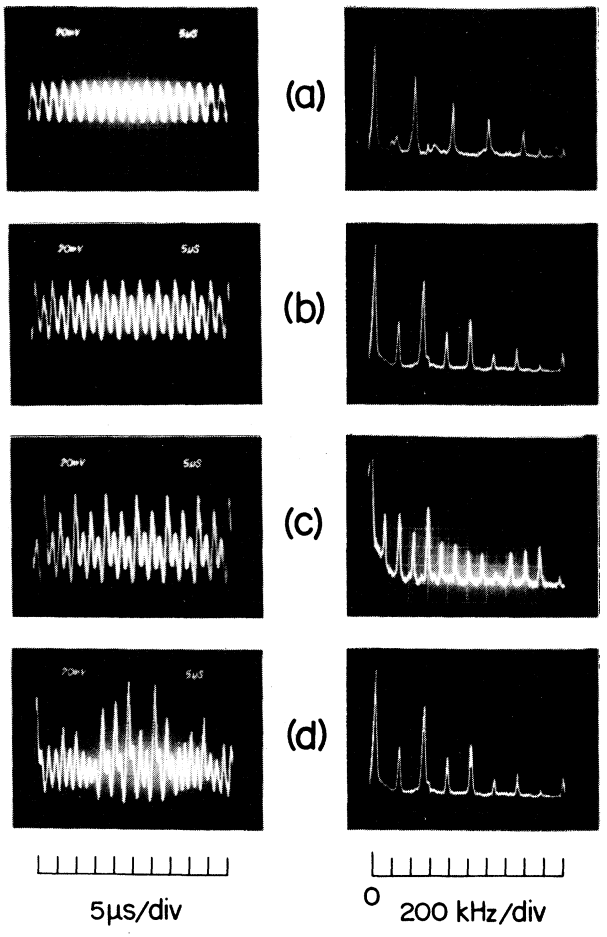

FIG. 1. Oscilloscope traces showing (a) period-1, (b) period-2, (c) period-4, and (d) chaotic oscillations and corresponding power spectra observed in perpendicular-pumping subsidiary resonance experiments at $R=h/h_c=2.12$, 2.19, 2.29, and 2.54, respectively (scenario F).

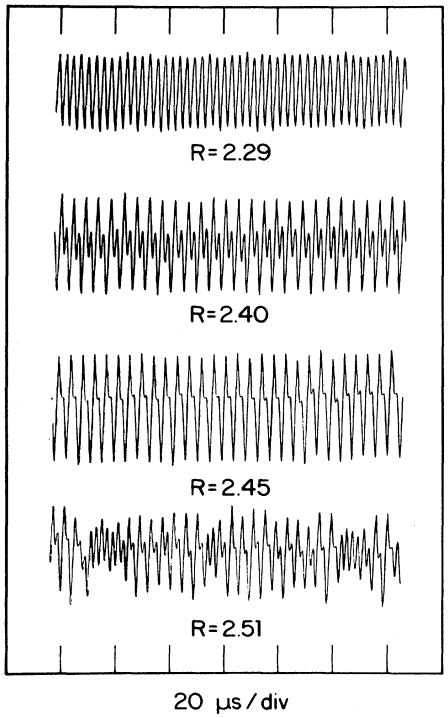

FIG. 2. Detected microwave absorption vs time corresponding to scenario C described in the text.

maximum at $R=2.45$, and loses its regularity above this value. Scenario C has also been previously reported in parallel pumping experiments,[7] observed with the sample axis [111] parallel to $\mathbf{H}_0$ and $H_0=1540$ Oe. This field value is very close to the minimum of the butterfly curve, at which the $\Theta_k=90°$ pair has wave vector $k\simeq 0$. In this configuration a nearly sinusoidal modulation first appears at $R\simeq 1.50$ and its frequency increases from the initial value of ~ 100 kHz linearly with R. A period doubling occurs at $R\simeq 1.62$, but there is no evidence of further bifurcations before the onset of chaos at $R=1.64$.

CHARACTERIZATION OF THE STRANGE ATTRACTORS

We have used the time-series data to characterize the chaotic attractors using the embedding technique. Two relevant quantities in this characterization are the dimensions and the Kolmogorov entropy. The dimension of an attractor is the first level of knowledge necessary to characterize its static properties and it is also a lower bound on the number of independent variables needed to model the dynamics. The Kolmogorov entropy K measures the loss of information on the initial conditions per unit time. Both quantities can be used to discriminate between stochastic and deterministic dynamical systems. For instance, the dimension of a limit cycle in the phase space is 1, whereas that of random noise is infinite. A regular trajectory has $K=0$, while white noise has $K=\infty$. For a deterministic chaotic system the fractal dimension, in general, holds a noninteger value and the Kolmogorov entropy has a finite positive value. A third set of quantitative measures of a strange attractor is represented by the Lyapunov exponents, but these cannot be reliably computed with the limited number of points in our time series. In order to obtain a reliable characterization of the attractors we have used two algorithms to calculate the dimensions, one proposed by Grassberger and Procaccia (GP) several years ago[21] and another introduced more recently[22] by Badii and Politi (BP).

In the GP algorithm one considers a time series $\{X_i\}_{i=1,\ldots,N}$ of points on the attractor and defines the correlation integral

$$C(r)=\lim_{N\to\infty}\frac{1}{N^2}\sum_{i\neq j}\Theta(r-|X_i-X_j|)\ , \tag{1}$$

where Θ is the Heaviside function. $C(r)$ may be calculated from a time series of a single physical quantity $x(t)$ (the voltage of the microwave diode detector in our case) with the embedding technique, by which E-dimensional vectors $X_i(t)$ are constructed with coordinates $x(t)$, $x(t+\tau),\ldots,x(t+(E-1)\tau)$, where τ is a fixed delay time and E the embedding dimension.[21] For a small r the correlation integral scales as

$$C(r)\sim r^d\ , \tag{2}$$

where the correlation exponent $d=\lim_{r\to 0}\log C/\log r$ is close to the fractal dimension of the attractor.

In the method of Badii and Politi[22] the central quantity is the moment of order γ calculated from the probability distribution $p(\delta,n)$ of nearest-neighbor distances δ among n randomly chosen points on the attractors

$$\langle\delta^\gamma\rangle\equiv M_\gamma(n)=\int_0^\infty\delta^\gamma p(\delta,n)d\delta\ . \tag{3}$$

From the scaling form of this as $n\to\infty$ one defines a γ-dependent dimension function

$$D(\gamma)=-\lim_{n\to\infty}\frac{\log n}{\log[M_\gamma(n)]}\ . \tag{4}$$

The dimension function yields, for specific γ values, several dimensions previously defined.[23] In particular, the fixed point $D_0=D(\gamma)=\gamma$ is the fractal dimension and $D_1=D(\gamma=0)$ is the information dimension, typically $D_0\gtrsim D_1$. The generalized metric entropies $K(\gamma)$ can be obtained from $D(\gamma)$. For $\gamma=0$ it satisfies the relation

$$\ln\langle\delta(n,E)\rangle\sim\frac{1}{D(0)}[\tau EK(0)-\ln n]\ , \tag{5}$$

where $\langle\delta(n,E)\rangle$ is the moment calculated from the E-dimensional embedded vectors and τ is the sampling time.

Strange attractors obtained from scenarios F and C described previously, both in the parallel pumping and subsidiary resonance processes, have been studied with the GP and BP methods. We present here details of the results obtained with the subsidiary resonance configuration at the onset of chaos ($R=2.51$) approached with scenario C previously described. The time-series data were obtained from the low-frequency amplitude modulation at intervals $\tau=0.2$ μsec, which is about one tenth of the fundamental period at $R=2.45$. Figure 3 shows the strange attractor of the trajectories projected on the $x(t)$-$x(t+\tau)$ plane. Figure 4(a) shows plots of $\log_{10}C(r)$ versus $\log_{10}r$ obtained with 2048 data points that are used to calculate the fractal dimension d with the GP algorithm. As the embedding dimension increases the slope of the curve in the range $-3<\log_{10}C(r)<-1$ converges to a value $d\simeq 1.6$. In the BP method we determine the dimension from plots of $\log_{1.18}\langle\delta\rangle$ for $\gamma=0$ versus $\log_{1.18}n$[24] shown in Fig. 4(b) for $E=1,2,\ldots,15$. For $E>6$ the slopes at the higher

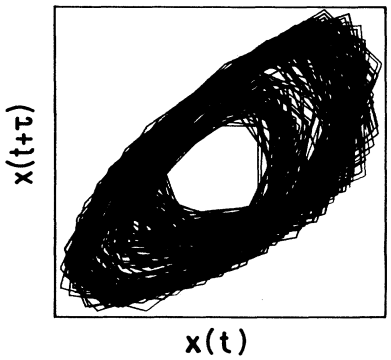

FIG. 3. Two-dimensional projection of the strange attractor at the onset of chaos in scenario C.

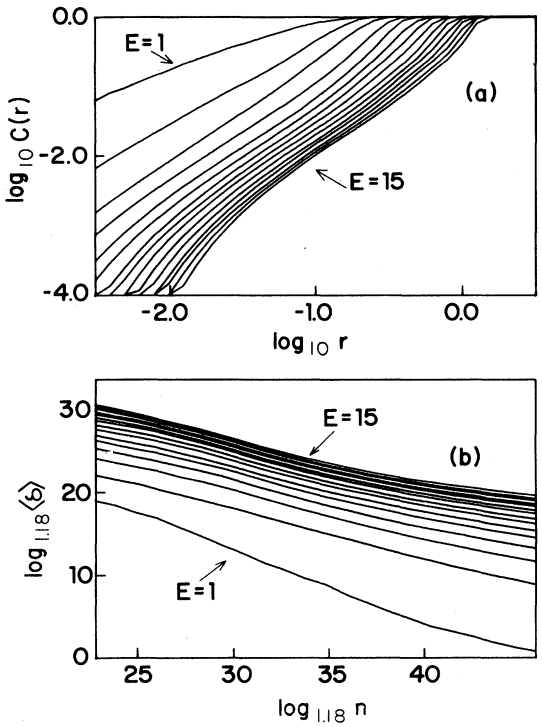

FIG. 4. (a) Correlation integral $\log_{10}C(r)$ vs $\log_{10}r$ calculated from the time-series data at the onset of chaos in scenario C. (b) Plots of $\log_{1.18}\langle\delta\rangle$ vs $\log_{1.18}n$ for $\gamma=0$ for several embedding dimensions (E) calculated from the same time-series data as (a).

$\log_{1.18}n$ end converge to a value for the information dimension $D_1\approx 1.5$, in good agreement with the dimension obtained with the GP method. The same procedure has been used to calculate the dimensions of the attractors with scenarios F in subsidiary resonance and C in parallel pumping. In all cases we find $1.4<d<1.8$, which is also close to the value obtained in YIG under parallel pumping at low temperature.[8]

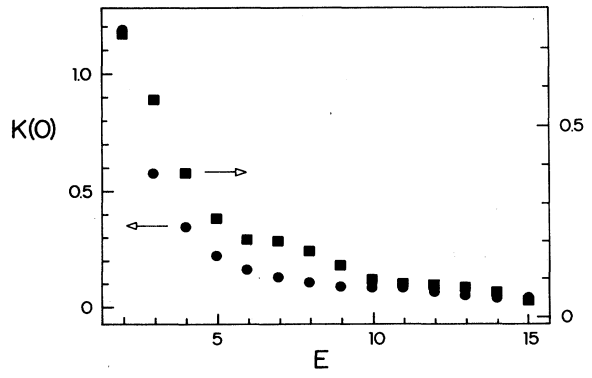

FIG. 5. Metric entropy vs the embedding dimension for the chaotic attractor at the accumulation point of scenarios F(●) and C(■).

From the time-series data we have also calculated the entropy $K(0)$ as a function of the embedding dimension using Eq. (5). Figure 5 shows the results at the onset of chaos in the subsidiary resonance. In both scenarios F and C, for large E the entropy converges to a constant value $K_c\simeq 0.05$. This positive constant value confirms the deterministic nature of chaos in our experiments.

DISCUSSION

Several conclusions can be drawn from the above results. The first is that the broad power spectra observed in spin-wave turbulence experiments is a manifestation of deterministic chaos. The chaotic state is observed only at selected experimental parameters, such as crystal orientation, static magnetic field (wave vector) value, and microwave pumping level. Different routes to chaos have been identified, both in the parallel pumping and the subsidiary resonance techniques. In all investigated experimental configurations the strange attractors at the onset of chaos have dimension $1.4\lesssim d\lesssim 1.8$. Somewhat higher dimensions have been obtained by other authors for materials[13] or configurations different from ours. This result indicates that despite the fact that a large number of magnon modes is excited above the instability threshold, the number of degrees of freedom is small, strongly suggesting that only a few spin-wave modes are involved in the chaotic dynamics. This is consistent with recent theoretical results[19,25] obtained with several simplifying assumptions (such as wave-vector-independent interaction and damping parameters). However, the nature of these modes remains to be clarified. Considering the fact that two- and three-mode models reproduce many features of the experimental observations, we believe that the dynamics is indeed governed by a few equations of motion describing collective spin-wave excitations. These collective excitations may result from the phase locking of many individual magnons into a small number of phase-locked modes, each one with a different phase. As shown by Lim and Huber,[20] when several magnons are phase locked, they are all described by just two equations of motion similar to those for one mode. This phase locking into collective modes would reduce the number of degrees of freedom. This interpretation is consistent with the fact that the self-oscillations obtained recently with numerical simulations using the two-mode model[7,17] are similar to earlier results involving a large number of modes.[26]

ACKNOWLEDGMENTS

The authors would like to acknowledge M. Warden and G. Broggi of the Physics Institute, University of Zurich, for providing the software in Ref. 24 and invaluable discussions. One of us (S.M.R.) acknowledges Prof. F. Waldner for the hospitality in Zurich and many stimulating discussions. This work has been supported by Financiadora de Estudos e Projetos, Conselho Nacional de Desenvolvimento Científico e Tecnológico and Coordenação do Aperfeiçoamento de Pessoal de Ensino Superior.

[1]T. S. Hartwick, E. R. Peressini, and M. T. Weiss, J. Appl. Phys. **32**, 223s (1961).
[2]H. Suhl, J. Phys. Chem. Solids **1**, 209 (1957).
[3]F. R. Morgenthaler, J. Appl. Phys. **31**, 95s (1960).
[4]E. Schlomann, J. J. Green, and U. Milano, J. Appl. Phys. **31**, 386s (1960).
[5]V. S. L'vov, S. L. Musher, and S. S. Starobinets, Zh. Eksp. Teor. Fiz. **64**, 1074 (1973) [Sov. Phys.—JETP **37**, 546 (1973)]; V. E. Zakharov, V. S. L'vov, and S. S. Starobinets, Usp. Fiz. Nauk **114**, 609 (1974) [Sov. Phys.—Usp. **17**, 896 (1975)]; V. I. Ozhogin and A. Yu Yakubovskii, Zh. Eksp. Teor. Fiz. **67**, 287 (1974) [Sov. Phys.—JETP **40**, 144 (1975)].
[6]G. Gibson and C. Jeffries, Phys. Rev. A **29**, 811 (1984).
[7]F. M. de Aguiar and S. M. Rezende, Phys. Rev. Lett. **56**, 1070 (1986).
[8]M. Mino and H. Yamazaki, J. Phys. Soc. Jpn. **55**, 4168 (1986).
[9]P. Bryant, C. Jeffries, and K. Nakamura in *Proceedings of the International Conference on the Physics of Chaos and Systems far from Equilibrium, Monterey, California, 1987* (North-Holland, Amsterdam, 1987), p. 25; Phys. Rev. Lett. **60**, 1185 (1988).
[10]S. M. Rezende, F. M. de Aguiar, and A. Azevedo, in *Magnetic Excitations and Fluctuations II,* edited by U. Balucani, S. W. Lovesey, M. G. Rasetti, and V. Tognetti (Springer-Verlag, Berlin 1987), p. 79.
[11]F. Waldner, D. R. Barberis, and H. Yamazaki, Phys. Rev. A **31**, 420 (1985).
[12]A. I. Smirnov, Zh. Eksp. Teor. Fiz. **90**, 385 (1986) [Sov. Phys.—JETP **63**, 222 (1986)].
[13]H. Yamazaki, M. Mino, H. Nagashima, and M. Warden, J. Phys. Soc. Jpn. **56**, 742 (1987).
[14]P. E. Wigen, H. Doetsch, Y. Ming, L. Baselgia, and F. Waldner, J. Appl. Phys. **63**, 4157 (1988).
[15]K. Nakamura, S. Ohta, and K. Kawasaki, J. Phys. C **15**, L143 (1982).
[16]X. Y. Zhang and H. Suhl, Phys. Rev. A **32**, 2530 (1985).
[17]S. M. Rezende, O. F. de Alcantara Bonfim, and F. M. de Aguiar, Phys. Rev. B **33**, 5133 (1986); J. Magn. Magn. Mater. **54-57**, 1127 (1986); Sergio M. Rezende and Flavio M. de Aguiar, Rev. Bras. Fis. **16**, 324 (1986).
[18]H. Suhl and X. Y. Zhang. Phys. Rev. Lett. **57**, 1480 (1986).
[19]T. L. Gill and W. W. Zachary, J. Appl. Phys. **61**, 4130 (1987).
[20]S. P. Lim and D. L. Huber, Phys. Rev. B **37**, 5426 (1988).
[21]P. Grassberger and I. Proccacia, Phys. Rev. Lett. **50**, 346 (1983); Physica D **9**, 189 (1983).
[22]R. Badii and A. Politi, Phys. Rev. Lett. **52**, 1661 (1984); J. Stat. Phys. **40**, 725 (1985).
[23]See, for example, J. D. Farmer, E. Ott, and J. A. Yorke, Physica D **7**, 153 (1983).
[24]R. Badii and G. Broggi, Physik-Institut der Universitat Zurich Software Report No. 6, May 1987 (unpublished).
[25]X. Y. Zhang and H. Suhl, Phys. Rev. B **38**, 4893 (1988); H. Suhl and X. Y. Zhang, J. Appl. Phys. **63**, 4147 (1988).
[26]V. S. L'vov S. L. Musher, and S. S. Starobinets, Zh. Eksp. Teor. Fiz. **64**, 1074 (1973) [Sov. Phys.—JETP **37**, 546 (1973)].

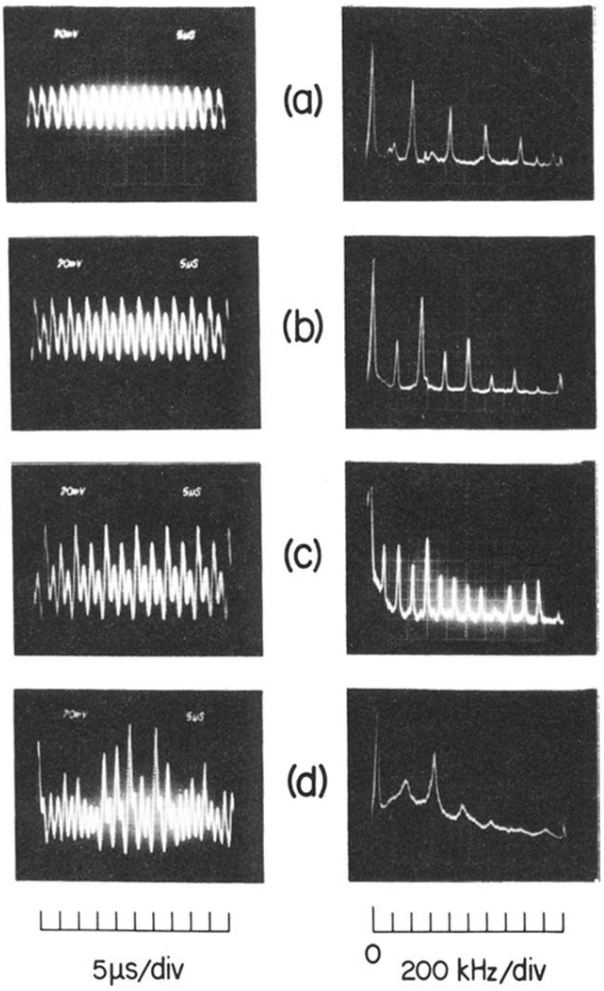

FIG. 1. Oscilloscope traces showing (a) period-1, (b) period-2, (c) period-4, and (d) chaotic oscillations and corresponding power spectra observed in perpendicular-pumping subsidiary resonance experiments at $R = h/h_c = 2.12$, 2.19, 2.29, and 2.54, respectively (scenario F).